

Pre-tapeout calibration and benchmarking of simulated neuron circuits

Philipp Dauer

Supervisor: Sebastian Billaudelle

December 28, 2019

1 Introduction

The leaky integrate-and-fire (LIF) model effectively captures the very core dynamics of a spiking neuron. Due to its simplicity it is predestined for neuromorphic implementations. To reproduce a more diverse set of biological firing patterns, the underlying differential equations must be augmented by additional terms. The adaptive exponential integrate-and-fire (AdEx) model (Naud et al. 2008) fulfils the equations

$$C \frac{dV}{dt} = -g_L(V - E_L) + g_L \Delta_T \exp\left(\frac{V - V_T}{\Delta_T}\right) + I_{\text{ext}} - w, \quad (1)$$

$$\tau_w \frac{dw}{dt} = a(V - E_L) - w, \quad (2)$$

where an exponential term and an adaptation current as an additional state variable w extends the LIF neuron model. The membrane voltage V of the LIF neuron model evolves according to the membrane capacity C and the conductance g_L as well as by an leak potential E_L and an external current I_{ext} . The exponential term, also scaled by the conductance g_L , represents a soft spiking threshold by using the threshold voltage V_T and the slope factor Δ_T . The adaptation current w drives the membrane voltage V as a additionally state variable. It is realised by a linearly coupled ordinary-differential-equation (ODE) with the adaptation time constant τ_w . A sub-threshold adaptation parametrized by the conductance a compares V with E_L .

A spike-triggered-adaptation mechanism and a reset

condition are given by

$$\text{If } V > 0 \text{ mV, then } \begin{cases} V \rightarrow V_r \\ w \rightarrow w_r = w + b. \end{cases} \quad (3)$$

The third prototype of the BrainScaleS-2 system introduced circuits for the emulation of the AdEx equations. A redesign is planned to overcome some of the limitations of the current design. The new circuits are designed to enable a truthful reproduction of the differential equations and to allow a straightforward calibration.

In the neuron, the exponential term is realised by an operational transconductance amplifier (OTA) as an input stage, is biased with $I_{b,\text{exp}}$ and comparing the membrane voltage V with E_{exp} . The output current is translated into a voltage, which is then applied to the gate of a transistor biased in the sub-threshold region. This transistor generates the exponential current as present in the differential equation.

The adaptation term is implemented as a low pass filter, consisting of an OTA, biased with $I_{b,\text{adapt}:\tau_w}$ and a capacitor. A sub-threshold adaptation is realised, again, by an OTA with bias current $I_{b,\text{adapt}:a}$, that compares V with E_L .

The performance of such neuron circuits can be assessed in dedicated benchmarks. A set of biologically inspired firing patterns have been suggested and analyzed in the context of the AdEx model Naud et al. 2008. These patterns seem particularly useful for benchmarking of our circuits.

To verify the circuit, calibration methods have to be found, that allow to transform biological parameters in to

hardware parameters. These transformations have to be based on measurements to determine the characteristic curves of the neuron circuits. Lookup mechanisms incorporating these curves and other already known properties of the circuits can then be used to find hardware parameters including bias currents and voltages etc. for the different firing patterns given by Naud et al. 2008.

The influence of transistor parameter variations, leading to local mismatch as well as differences in the parametrization of individual neuron instances, is analyzed in Monte Carlo simulations. The circuits are simulated with *Cadence Spectre*, which is steered via the *teststand* Python package. This package supports the parallel execution of multiple simulation runs, which accelerates the measurements for larger numbers of Monte Carlo samples.

2 Calibration methods

The calibration of the neurons circuit to the biological parameters from the firing patterns plays a leading role in this internship. We assume, that a one-to-one connection between the bio parameters and the currents and voltage of the circuits exist. To be more efficient in time and cost, the calibration is physically divided in a measurement part and a apply or rather a resolve part. In the measurement part of the calibration, special firing or sub-threshold patterns are stimulated and recorded during one voltage or current is changing. In the easiest case it is possible to calculate directly without other dependencies an according parameter. This data is saved in a database. Right before the simulation, different functions find from the current/voltage-parameter-mapping the right currents and voltages according to the desired firing pattern. This resolve part takes the saved data as well as hardware parameters that includes the speedup factor of BrainScalesS $\alpha_t = 1000$, a voltage mapping factor $\alpha_v = 15.0$ with an offset voltage of 1.5V and a capacity factor $\alpha_c = \frac{C_{hw}}{C_{bio}}$, with a hardware capacity C_{hw} and a biological suggested capacity C_{bio} . To focus more on the methods than on the actual implementation, in the following description both elements of calibration

are discussed together. The general setting of the tool was given by Johannes Weis, especially he implemented a simulation class and sub-classes for parameter sweeps and binary searches, that allows multi threading by using *teststand*. He also invented a assess from python classes to a .json database. His work allows to set and measure or rather simulate a lot of neuron-samples at the same time.

Finally, firing patterns are simulated in an independent tool, that allows a apply parameters and the stimulus of different patterns, run them in parallel and plot as well as save the results. For applying, it is possible to hand in bio parameters or fixed values some or all of the voltages and currents of the circuit. Bio parameters will be calibrated with the resolve routines, if already a fixed value is given, the calibration will be overwritten. For comfort, it is possible to run select able sets of neurons and the simulation uses multi threading classes of Johannes Weiß, that interacts with *teststand* and through this with *Cadence Spectre*.

2.1 Input offset of the sub-threshold adaptation

As written in the introduction, the sub-threshold adaptation, given by the parameter a and adjusted by the current $I_{b,adapt:a}$ uses an OTA to compare the membrane voltage V with the leak voltage E_L . Due to manufacturing reasons the OTA has an offset voltage, that has an impact on the adaptation- and membrane voltage. To deal with this well known issue, the OTA is not wired to E_L but to

$$E_{off,adapt:a} = E_L + \Delta E, \quad (4)$$

where ΔE represents the offset. Together with the assumption, that this offset is independent of $I_{b,adapt:a}$, a simple binary search find an adaptation voltage V_w with activated a -OTA (e.g. $I_{b,adapt:a} = 0.2 \mu A$), that is similar to a target, that is measured with deactivated a -OTA ($I_{b,adapt:a} = 0$). Target as well as binary search measurement time should be long after the adjustment of the parameters. It is possible to set negative a -values in the AdEx neuron model. To realise this in the circuits, a

switch `invert_a` with binary input is given and makes it necessary to repeat this measurement with this second case. Both measured results are saved in the database. A resolving takes just this offset result, for an applying due to the desired firing pattern, equation [4] solves the parameter $E_{\text{off,adapt:a}}$ directly.

2.2 Adaptation time constant

As written in equation 2, the adaptation depends on an adaptation time constant τ_w . The rules for a RC element says, that

$$\tau_w = \frac{C_w}{g_{\tau_w}(I_{\text{b,adapt}:\tau_w})}. \quad (5)$$

So the hardware given capacity and the adjustable conductance, realised by an OTA, changes the adaptation time constant. This τ_w -OTA has two different outputs and in particular two different linear dependent conductances,

$$\underbrace{g_{\text{adapt}}}_{\text{adaptation on } V} = 12 \cdot \underbrace{g_{\tau_w}}_{\text{feedback loop}}, \quad (6)$$

to reach a good fitting ratio between the parameters for the adaptation time constant and the sub-threshold adaptation. To measure this adaptation time constant, a spike is triggered and a fit

$$V^*(t, I_{\text{b,adapt}:\tau_w}) = a \cdot \exp\left(\frac{-t}{\tau_w(I_{\text{b,adapt}:\tau_w})}\right) + b, \quad (7)$$

where V^* is the membrane potential after a spike occurs, gives a τ_w . This is repeated for different values of $I_{\text{b,adapt}:\tau_w}$. To get good results, $I_{\text{b,adapt:a}} = 0.0e^{-6}A$ and $I_{\text{b,adapt:b}} = 1.0e^{-6}A$ so that a well sized charge is loading the adaptation capacity C_w more or less instantaneous after the spike. The pairs of vales of τ_w and $I_{\text{b,adapt}:\tau_w}$ are saved in the database. For resolving all this measured data are fitted by a function

$$\tau_w = \sum_{i=1}^4 a_i \cdot I_{\text{b,adapt}:\tau_w}^{-i}, \quad (8)$$

with fitting coefficients a_i . Now a simple binary search is able to find the right $I_{\text{b,adapt}:\tau_w}$ for a given target τ_w .

2.3 Sub-threshold adaptation

In her master thesis (Kriener 2017), Laura Kriener wrote about a similar sub-threshold adaptation of a AdEx neuron. She defined $\Delta := (V - E_L)$ as a membrane voltage change caused throw a a sub-threshold stimulus. If this membrane voltage change is also influenced by an sub-threshold adaptation, she called it Δ_a . Kriener discovered, that the sub-threshold adaptation is given by

$$a = g_L \cdot \left(\frac{\Delta}{\Delta_a} - 1\right), \quad (9)$$

where a or rather Δ_a are dependent from $I_{\text{b,adapt:a}}$. In a baseline measurement, the

$$\Delta = V_{[\text{pre stimulus}]} - V_{[\text{stimulus}]} \quad (10)$$

and

$$g_L = \frac{C_m}{\tau} \text{ with fit function } V(t) = a \cdot \exp\left(\frac{-t}{\tau}\right) + c \quad (11)$$

are determined. Recording the Δ_a against $I_{\text{b,adapt:a}}$, the equation [9] solves a against $I_{\text{b,adapt:a}}$. This value pairs are saved in the database. The resolve function takes this values and uses a polynomial fit of the fourth degree to discribe them. To get a specific $I_{\text{b,adapt:a}}$ for a given a , a implemented routine searches a root in a certain $I_{\text{b,adapt:a}}$ -range of the fit minus the given target a .

2.4 Spike-triggered adaptation

In equation [3], the reset condition including a spike-triggered adaption is described. Realised in circuits, a current $I_{\text{b,adapt:b}}$ takes nearly instantaneous in a short period δt of time a charge q on the capacity C_w or rather on w . The resulting current $I_{\Delta vb}$, caused by this voltage jump Δvb , is described by

$$b = I_{\Delta vb} = g_{\text{adapt}}(\tau_w) \cdot \Delta vb(I_{\text{b,adapt:b}}). \quad (12)$$

The voltage jump Δvb is determined for many $I_{\text{b,adapt:b}}$ and saved in the database. Afterwords they are fitted by an polynomial function of second degree. A resolve function computes first a target- Δvb from a given b and

τ_w using equation [6] and

$$\Delta v b_{\text{target}} = \frac{b_{\text{target}}}{g_{\text{adapt}}} = \frac{b_{\text{target}}}{12 \cdot g_{\tau_w}} = \frac{b_{\text{target}} \cdot \tau_w}{12 \cdot C_w}. \quad (13)$$

The factor 12 between g_{adapt} and g_{τ_w} is well known and tested. By using a binary search, the resolve function gives a $I_{b,\text{adapt}:b}$ for a with equation [13] solved $\Delta v b_{\text{target}}(b, \tau_w)$.

2.5 Exponential term

As described in equation [1], the threshold is given by an exponential term, which is parameterized by g_L , Δ_T and V_T . Due to the technical realisation of the circuits, output current I_{exp} of the exponential fulfils the equation

$$I_{\text{exp}} = a \cdot e^{\frac{v_m}{b}}, \quad (14)$$

with parameters $a(E_{\text{exp}}, I_{b,\text{exp}})$ and $b(I_{b,\text{exp}})$. The current is calculated from

$$I_{\text{exp}} = C_m \cdot \frac{dV_m}{dt} \quad (15)$$

for some $I_{b,\text{exp}}$. With a second degree hyperbolic fit of b , that can be identified as Δ_T (c.f. [1]), the dependency form $I_{b,\text{exp}}$ is determined. Given a specific Δ_T and V_T configuration, $I_{b,\text{exp}}$ is given by a binary search on the parameter b . In a next step, a can be identified by

$$a = g_L \cdot \Delta_T \cdot e^{\frac{-V_T}{\Delta_T}}. \quad (16)$$

The circuit given equation

$$a(I_{b,\text{exp}}, E_{\text{exp}}) = \hat{I} \cdot e^{\frac{-I_{b,\text{exp}}}{b(I_{b,\text{exp}})}}, \quad \hat{I} = \text{const}, \quad (17)$$

in mind, a as well second degree hyperbolic fit on $I_{b,\text{exp}}$ and a , gives a fitting \tilde{a} to the calibrated $I_{b,\text{exp}}$. With equation [17], that grants a constant \hat{I} , and E_{exp}^{\sim} , that was set at the measurements, the equation

$$E_{\text{exp}} = E_{\text{exp}}^{\sim} + b \cdot (\log \tilde{a} - \log a), \quad (18)$$

with a calculated by [16] calculates E_{exp} . To improve the robustness of the algorithm, I_{exp} is measured for more

then one *ve xp*.

2.6 Leak calibration

Unfavorably, we determined that on the one hand the sub-threshold adaption offset is not independent of $I_{b,\text{adapt}:a}$ as assumed in equation [4] and on the other hand a significant offset of the time-adaption-double-OTA has a significant impact on w . It is clear, that this issue can be fixed by a calibration as done before. Due to a limited time, we decided to solve this issue for now in a simple but time inefficient way. When the calibration to the parameters of a firing pattern is applied, a binary search without a stimulus set E_L to

$$E_L = E_L + \text{offset}, \text{ so that } V_{[\text{resting}]} = E_L. \quad (19)$$

The determined E_L will be applied.

3 Results

3.1 Quality of calibration

To verify the quality and the independence of the calibration, some tests are done for a , b , τ_w and the exponential term calibration. Therefore each of this calibration methods got some target bio parameter of pattern, that are similar to the calibration measurement pattern. After simulating them, similar routines like used for calibration are used to extract bio parameters back from the traces. This is done for a one-to-one sweep of the calibrated parameters them self, but also if possible in dependency of other parameters. The results are determined for 50 neuron samples.

Due to a look on sub-threshold calibration (fig. 1), the dependency of τ_w was tested, because τ_w couples the adaptation term back to the membrane. It can be recognised, that high a -values as well as long adaptation time constants has a considerable impact on the precision of the calibration. A drift to smaller a -values can be observed.

With the same argument as used in the sub-threshold adaptation, the dependency of τ_w to the spike triggered adaptation (fig. 2) was determent. In difference to the

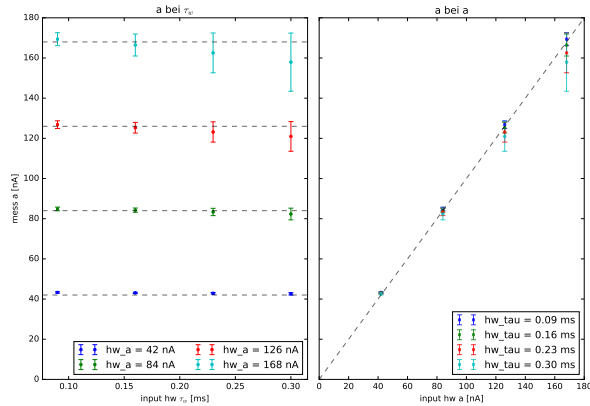


Figure 1: sub-threshold adaptation calibration results in dependency of the adaptation time constant τ_w and an given input a .

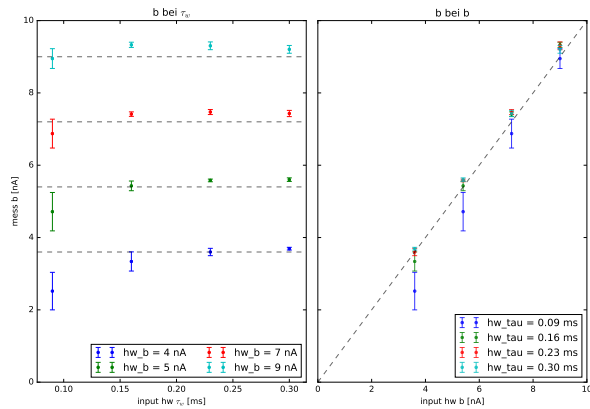


Figure 2: spike triggered adaptation calibration results in dependency of the adaptation time constant τ_w and an given input b .

sub-threshold adaptation, the spike triggered adaptation are just deviate significant for very short adaptation time constants.

Due to the determent method for the adaptation time constant (fig. 3), useful dependencies on τ_w can't be measured. Never the less, the adaptation time constant fits well on the identity function.

Until now, a direct testing of the exponential term calibration failed. It was planed, to measure Δ_T and V_T with respect to different target Δ_T , target V_T and target g_L . This plan failed, because the measurement routine used in the calibration measurement method needs spiking patterns to calculate the current, which the ex-

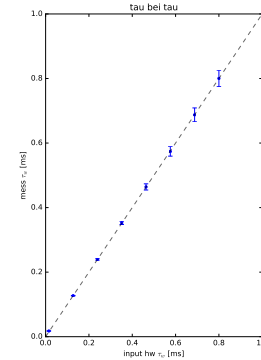


Figure 3: adaptation time constant calibration results

ponential term append to V . But even if this would be managed, the results would have huge uncertainties due to realistic small g_L values. Never the less, the pattern reproduction shows, that the exponential term is well calibrated.

3.2 Firing patterns

As described above, we have a tool, that allows to calibrate and simulate one or multiple neurons in parallel for different patterns. This is used to do the benchmark test of the circuits and a numeric solution of equation [1] gives a direct classification of the calibration and simulation results. This benchmark test comprises initial bursting, regular bursting, delayed spiking and accelerating, delayed regular bursting and transient spiking and should show, whether the circuits works and whether we understand truly, how circuits operate and how we bias them right. A major problem of the benchmark test is, that the numeric solution with parameters from Naud et al. 2008 for transient spiking does not show a transient spike but a permanently bursting. Also his firing pattern for delayed regular bursting does not seems correct, because not even a single spike occurs. This in mind, Kriener 2017 used the figures with firing patterns from Naud et al. 2008, but chosed some different parameters. She succeeded in finding parameters for the transient spiking, but failed with delayed regular bursting. On the other hand, Kriener 2017 used parameters for delayed accelerating, that does not show even a single spike. Also her regular bursting is more delayed then the firing pattern

of Naud et al. 2008.

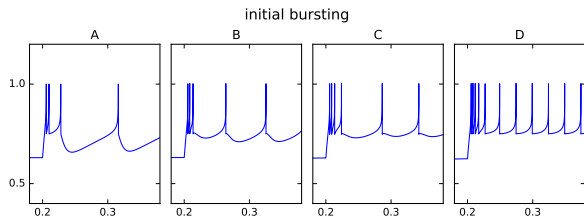


Figure 4: Membrane potential during the initial bursting firing pattern with parameters from Naud et al. 2008. A: numeric solution, B: neuron 28 simulation as example for a well matching neuron, C: neuron 21 simulation as example for a quadra initial burst with delayed last spike and D: neuron 19 simulation as example for an always bursting neuron. Plots has on x axis time in milliseconds and on y axis membrane potential V in volt.

Starting with the initial bursting firing pattern by Naud et al. 2008, the initial burst has one case of double spike bursting, 17 cases of triple spike bursting (fig. 4B), 29 cases of quadra spike bursting (fig. 4C) and three cases with an initial burst with more than four spikes. In 26 of 50 cases, the last spike of the initial burst limps with the other spikes. During the following repetitive single spiking, two samples burst, 30 samples spikes faster than the numeric solution and one neuron slower as well as 17 samples are spiking with the right speed. Two neurons are saturating (fig. 4D), but the majority of samples has a dynamic range between 0.2 V and 1 V.

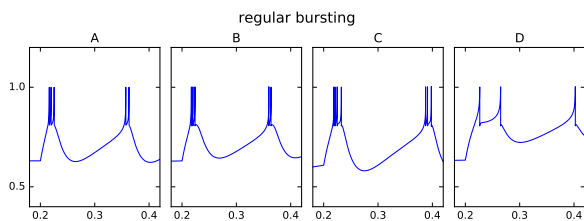


Figure 5: Membrane potential during the regular bursting firing pattern with parameters from Naud et al. 2008. A: numeric solution, B: neuron 4 simulation as example for a well matching neuron, C: neuron 35 simulation as example for a quadra initial burst with delayed last spike and D: neuron 3 simulation as example for a single spiking neuron. Plots has on x axis time in milliseconds and on y axis membrane potential V in volt.

Analysing results from regular bursting firing pattern

with the parameter set given by Naud et al. 2008, the huge majority of neuron samples does show the right spiking characteristic. Usually the repetitive bursts has one spike less than the initial bursts of a sample. Even, if one sample shows just a double spike initial bursting and a single spiking in the following (fig. 5D), 26 of in total 50 neurons have a triple spike initial bursting (fig. 5B) as given also by the numeric solution (fig. 5A). Another 12 neuron samples show a quadra spike initial burst (fig. 5C) and in total 10 samples show a limping last spike of the initial burst. Looking on the repetitive bursts of this pattern, 37 double spike bursting neurons and 12 triple spike bursting neurons can be counted. Most often a lower frequency of the burst then given by the numeric solution can be observed, so the right timing is counted 28 times and a lower frequency 21 times. Just one neuron samples shows a higher frequency of the bursts. Finally no saturation can be determent and the dynamic range of w starts at 300 mV and end at 600 mV.

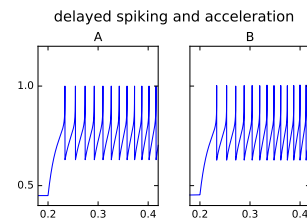


Figure 6: Membrane potential during the delayed spiking and acceleration firing pattern with parameters from Naud et al. 2008. A: numeric solution, B: neuron 10 simulation as example for all other tested neurons. Plots has on x axis time in milliseconds and on y axis membrane potential V in volt.

The simulation of the delayed spiking and acceleration (fig. 6B), with parameters given by Naud et al. 2008, succeeded in all 50 cases. All samples are delayed for the same order of time as given by numeric solution (fig. 6A). Looking on details, small differences between the acceleration can be observed, which can be interpreted by small differences in the decreasing of the adaptation potential w , which dynamic range starts at 900 mV and ends at approximately 200 mV.

The simulation of the delayed regular bursting, using a new created parameter set as given in the Appendix,

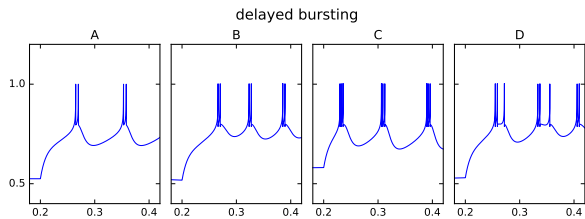


Figure 7: Membrane potential during the delayed regular bursting firing pattern with modified parameters to match to the figure from Naud et al. 2008. A: numeric solution, B: neuron 16 simulation as example for a well matching neuron, C: neuron 19 simulation as example for less delayed and triple burst firing pattern and D: neuron 14 simulation as example for a delayed last spike of a burst neuron. Plots has on x axis time in milliseconds and on y axis membrane potential V in volt.

succeeded in 45 of 50 cases in a way, that clearly a delaying and a repeated bursting occurs. In contradistinction to the numeric solution, in 40 of this cases not a double spike burst, but a triple spike burst can be observed. The five not matching samples are divided up in one neuron, that does only delayed single spiking and four neurons, that show a double spike burst, but third single spike, that follows the burst. All samples are delayed, just 14 has an occurring time, that is half the numeric solution. The dynamic range of w is determined between 350 mV and 600 mV.

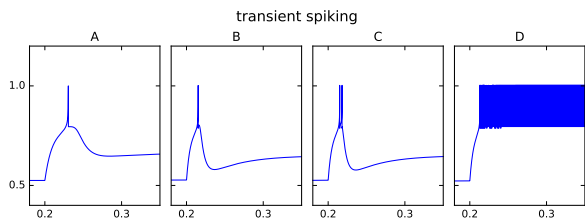


Figure 8: Membrane potential during the transient spiking firing pattern with parameters from Kriener 2017. A: numeric solution, B: neuron 41 simulation as example for a well matching neuron, C: neuron 4 simulation as example for a double spiking neuron and D: neuron 28 simulation as example for a w saturation expressed by permanent bursting. Plots has on x axis time in milliseconds and on y axis membrane potential V in volt.

Last but not least, the simulation of a transient spiking firing pattern with parameters from Kriener 2017 shows

in 24 times a single spike (fig. 8B) as also given by the numeric solution (fig. 8A). In just one neuron sample no spike occurs, but 24 times a double spike can be observed (fig. 8C). This can be interpreted as a strong dependency on the stimulus current. 4 times constantly bursting happened, the same neurons shows also a saturation of w . The timing of 12 neuron samples is delayed compared to the numeric solution, other 37 neuron samples are timed right. The dynamic range of w is limited by its initial state and causes four neurons samples of constant bursting (fig. 8D). It usually can be determined between 400 mV and 800 mV.

4 Discussion and outlook

The benchmark testing of the circuits has shown that all relevant and important firing pattern can be reproduced in their characteristic structure in nearly all tested 50 cases. Sometimes the the circuits have a tendency to saturate in the adaptation membrane potential w . In this cases the neurons fire constantly. Also, in other cases, it can be observed, that the neurons spikes more often than a numerical simulation of the differential equations do. Keeping in mind, that the given firing pattern does not necessarily represent a robust choice of parameters but a small piece of the phase space of parameters, this is not a major problem. The firing patterns represent a rather demanding benchmark, so this behavior was not unexpected.

Never the less we can expend the testing to get a better knowledge about the behavior of the circuits. This could include on the one hand to find robust parameters with a qualitatively similar behavior than the now used parameters for the firing patterns and also to simulate more Monte Carlo samples of the circuit. On the other hand, this should include more than AdEx extensions, so e.g. different E_L or V_r . The virtual infinite reset conductance is not realistic. Also the offset of the τ_w -OTA should be calibrated with all its dependencies.

Even not discussed before in detail, the circuit's dependency on temperature was investigated. We performed simulations for 40 °C and 60 °C and received accept-

able result for the adaptation term, just the exponential term is exponential term is influenced. These effects can clearly be compensated by providing calibration data for multiple operating temperatures. The exponential term circuit also includes a compensation mechanism, which was not used thus far.

Another aspect is the digital-analog-converter (DAC) has a finite resolution. So it would be interesting to test the simulation of the benchmarks with rounded calibration values. Also a simulation with noise on the parameters is conceivable. All this could have an impact on the results of the benchmark test and could give new impressions on the circuits. To simulate more neurons, it is planned to clean up the calibration and simulation code for CI (Jenkins). The last step would to implement the circuits on the next chip generation.

5 Appendix

See table 1.

References

- Kriener, Laura (Mar. 2017). “Characterization of Single-Neuron Dynamics in the Development of Neuromorphic Hardware”. MA thesis. Heidelberg University.
- Naud, Richard et al. (2008). “Firing patterns in the adaptive exponential integrate-and-fire model”. In: *Biological cybernetics* 99.4-5, p. 335.

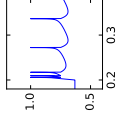
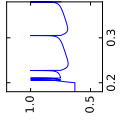
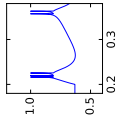
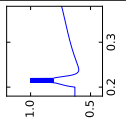
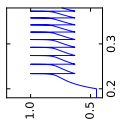
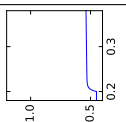
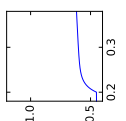
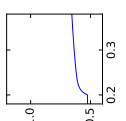
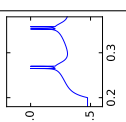
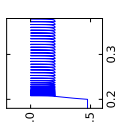
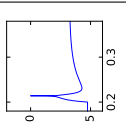
	initial bursting		regular bursting		delayed accelerating		delayed regular bursting			transient spiking	
	A	B	A	B	A	B	A	B	C	A	B
C (pF)	130	130	200	200	200	200	200	100	100	100	100
g_L (nS)	18	26	10	40	12	40	12	20	10	10	20
E_L (mV)	-58	-58	-58	-58	-70	-70	-70	-65	-65	-65	-65
V_T (mV)	-50	-50	-50	-50	-50	-50	-50	-50	-50	-50	-50
Δ_T (mV)	2	2	2	2	2	2	2	2	2	2	2
a (mS)	4	4	2	2	-10	-10	-6	-10	-8	-10	15
τ_w (ms)	150	150	120	120	300	300	300	90	90	90	90
b (pA)	120	120	100	100	0	0	0	30	50	30	300
V_r (mV)	-50	-50	-46	-46	-58	-58	-58	-47	-47	-47	-47
I_{ext} (pA)	400	400	210	410	300	210	110	110	110	350	350
											

Table 1: Collection of AdEx firing patterns from A: Naud et al. 2008 and B: Kriener 2017. Pattern C was a result of modifying the parameters such that they are match figures in Naud et al. 2008 by Sebastian Billaudelle and Philipp Daur. Plots has on x axis time in milliseconds and on y axis membrane potential V in volt.